ELSEVIER

Polymer 41 (2000) 4285–4289

polymer

Surface morphology and crystallinity of biaxially stretched PET films on the nanoscale

F. Dinelli, H.E. Assender, K. Kirov, O.V. Kolosov*,[1]

Department of Materials, University of Oxford, Parks Road, Oxford OX1 3PH, UK

Received 17 June 1999; accepted 9 July 1999

Abstract

The surface morphology and crystallinity of biaxially drawn (BD) and amorphous poly(ethylene terephthalate) (PET) films were investigated by means of scanning probe microscopy. The PET surface is best imaged using non-contact mode atomic force microscopy (NC-AFM). Contact mode (C-AFM) under water can also offer a good resolution but the PET surface is not stable for long periods under such conditions.

The BD film texture appears to be made up of "hillocks" of about 20 nm in diameter, while amorphous PET films appear featureless. It seems plausible to suggest that the observed hillocks represent small crystallites formed during the production process of BD films.

Keywords: Poly(ethylene terephthalate); Scanning probe microscopy; Crystallinity

1. Introduction

Biaxially drawn (BD) poly(ethylene terephthalate) (PET) films with a barrier coating are widely used for packaging applications, however many of the surface properties of the polymer on which the barrier coating is deposited are not well characterised. The morphology and the crystallinity of the surface of a BD PET film is of general interest in the study of polymer surfaces and it is also of importance for understanding the nature of barrier film growth. Crystallisation of amorphous PET by heating and/or stretching amorphous films has been extensively studied by techniques sensitive to bulk properties such as differential scanning calorimetry (DSC) [1–3], X-ray diffraction [4,5], and infrared spectroscopy [6,7]. Electron microscopy has been also used to investigate crystallisation: spherulites and lamellae have been clearly imaged [1,8–10]. As a surface investigation technique, atomic force microscopy [11] (AFM) can offer a spatial resolution comparable to electron microscopy without the need of complex sample preparation and without concerns of 'beam damage' of the sample [12]. For example, the morphology and formation of lamellae have been extensively characterised for poly(ethylene) (PE), poly(ethyleneoxide) (PEO) and other polymers [13–16]. In addition, scanning probe microscopy has the capability to probe surface mechanical properties [17,18]. However, the few investigations on BD PET films by AFM reported in the literature have not addressed the problems of nanoscale surface morphology and crystallinity. Most of these papers deal with the deformation induced when using contact mode AFM (C-AFM) [19,20]. Ling et al. [20,21] presented a study of deformation induced by C-AFM and proposed the use of non-contact AFM (NC-AFM) in order to avoid such damage. However, their work addressed mostly the applicability of AFM for surface analysis of polymers without trying to interpret the surface texture on the nanoscale level and attempt to distinguish crystalline from amorphous phases.

In an attempt to identify the crystalline phase, Gould et al. [19,22] presented images with very elongated features, which they interpreted as lamellae. This interpretation is not quite convincing, as the cross-section dimensions of these features are larger than one would expect for lamellae.

This paper describes the outcome of studies of the surface structure and establishes a few milestones for future investigations.

2. Experimental

The samples investigated in this work were BD films

* Corresponding author. Tel.: +44-1865-273735; fax: +44-1865-273789.
E-mail address: oleg.kolosov@materials.ox.ac.uk (O.V. Kolosov).
[1] Present address: SYMYX Technologies, 3100 Central Expressway, Santa Clara, CA 95051, USA.

0032-3861/00/$ - see front matter
PII: S0032-3861(99)00500-5

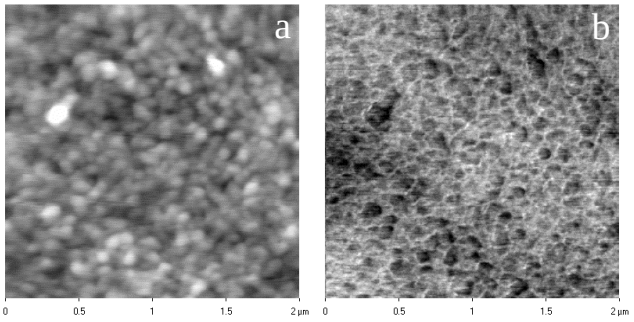

Fig. 1. BD PET film: (a) C-AFM image in air at 0 nN load, RMS = 1 nm; (b) LFM image. It can be noticed that there is a strong contrast in the LFM image (dark regions correspond to the regions of less friction). The C-AFM image remains stable unless one applies a higher load. The texture appears made of larger features compared to Fig. 2.

(12 μm thick) and amorphous PET films (Goodfellow, 300 μm thick). In order to avoid modification of the polymer morphology, the surface of the films was not cleaned (for example, by plasma treatment) prior to the AFM analysis.

A number of heat-treated (HT) samples were prepared by annealing the amorphous PET at various elevated temperatures in the range 120–220°C with the sample constrained to avoid contraction and to keep the sample flat. The amorphous film, which was initially transparent, became opaque in all cases after the heat treatment as a result of crystallisation that takes place. Attenuated total reflection (ATR) was used to characterise the surface crystallinity. The films were characterised using Fourier transform infrared (FTIR) spectrometry with spectra measured on a Perkin–Elmer Spectrum 2000 Explorer FTIR spectrometer at a resolution of 4 cm^{-1} and co-addition of 120 scans.

For the morphology studies of polymer surfaces, we have used a commercial AFM (CP model, Park Instruments). This system allows one to work in the conventional C-AFM and NC-AFM in air. When using C-AFM, the system also allows operating in lateral force microscopy (LFM) mode [23]. LFM is commonly used to investigate frictional properties, which are generally related to compositional differences of the surface [24,25]. One can modify the basic set-up to allow working under liquid [26] (water or *n*-heptane, for instance). For this purpose, we have built a small liquid cartridge, as the commercial one revealed was not to be mechanically stable. The AFM tip and sample are fully immersed under liquid, preventing the formation of a water meniscus between tip and surface, typical for C-AFM in air. This meniscus is associated with an attractive force between tip and surface that is detrimental to a non-invasive functioning of the AFM especially when investigating compliant and weak surfaces.

In an attempt to distinguish the crystalline from the amorphous phase, force modulation microscopy [17] (FMM) and ultrasonic force microscopy [27] (UFM) techniques were employed. FMM is a technique widely used for polymeric samples [28–30]. In a C-AFM set-up, the tip or the surface position is modulated at low frequency, and the cantilever response is collected as a measure of the contact compliance. UFM is a recently developed technique in which the sample is vibrated at ultrasonic frequency. Originally developed to overcome the limitations of FMM at high stiffness values, UFM has also proved to be useful for relatively compliant materials such as polymers [31,32]. UFM has also shown another very useful feature: it reduces the surface damage when operating in contact mode, as the tip-surface contact is temporarily broken for a fraction of every ultrasonic cycle [33].

In all AFM studies presented here, Ultralevers™ (Park Instruments, USA) made of silicon, triangularly shaped and of various dimensions were used. The cantilevers used for the C-AFM have nominal spring constant ranging between 0.16 and 0.24 $N\,m^{-1}$, and nominal tip radius of 10 nm. Cantilevers used for the NC-AFM have nominal spring constant ranging between 1.1 and 1.6 $N\,m^{-1}$, and nominal tip radius of 10 nm.

3. Results and discussion

The first approach was to use C-AFM in air while setting the working load at very low values. The load can be set to a negative value because of the meniscus, which forms between tip and surface creating an attractive force. Therefore, one can work with the cantilever negatively bent, though there is still a positive force acting between the tip and the sample. From the beginning, it was clear that the BD film surface was weak and not able to sustain the normal and the shear load due to tip dragging. One can deform the surface in various ways: in general, increasing the load increases the damage. The damage can be quantified by measuring the root mean square (RMS) roughness of the surface investigated before and after scanning at various loads. The formation of bundles and its dependence on scanning speed have already been reported in literature and were not within the scope of this work. As already mentioned in previous studies, UFM proved quite powerful in reducing damage on polymeric samples. Unfortunately, in this case, this technique was not beneficial in avoiding surface damage.

Under particular conditions not identified explicitly but which appeared to be related to the tip shape and relative humidity of the environment, it was possible to image the surface in the C-AFM mode with no apparent damage. The RMS value remained in a relatively restricted range (1–2 nm). However, even in these cases, there were some hints that the surface had been modified. For instance, the first scan line seemed to be different from the following ones which however stabilised almost immediately. Unfortunately, our system cannot work in a single line scan mode: the sample is continuously scanned back and forward immediately after the approach. Fig. 1 shows C-AFM and

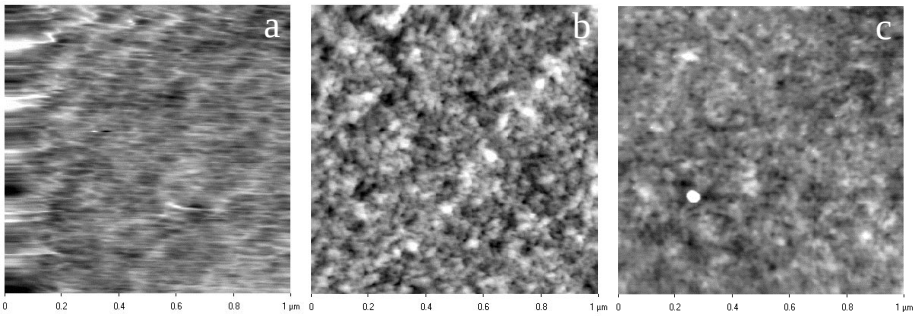

Fig. 2. BD PET film: (a) C-AFM image in air at 0 nN load, RMS = 1.6 nm; (b) C-AFM image under water at 0 nN load, RMS = 1.5 nm; (c) NC-AFM image, RMS = 1.2 nm. Note the finer structural details that are observable in (b) and (c).

LFM images of a BD PET film in which the image shown in Fig. 1 was quite stable in time unless the load was increased. The RMS roughness had a value of 1 nm. There was no clear evidence of damage induced by tip dragging. The LFM image (Fig. 1(b)) shows a contrast, which suggests that the surface was not homogenous but presented areas of different frictional behaviour. The darker areas in the image correspond to regions of relatively low friction. This observation was repeated on different areas and with different tips. Zooming out did not show any damaged area. Evidence that some damage was actually occurring was found when comparing these results with those from working in contact mode under liquid and in non-contact mode.

Fig. 2 compares three images of a BD film obtained working in C-AFM in air and under water, and in NC-AFM. In this case, the C-AFM image shows clearly that damage has occurred. This modification must be restricted to the first few angstroms of the surface as the RMS value does not vary dramatically between the different techniques and is still comparable to the one obtained for Fig. 1(a). The C-AFM image under water and NC-AFM images show a more detailed texture compared to Fig. 1(a). One more interesting observation is that the LFM contrast vanishes when working under water or *n*-heptane, suggesting that a thin liquid film is formed between the AFM tip and the polymer surface under liquid AFM imaging. We can conclude from this that, a modification of the surface (albeit a shallow one) was induced in the area shown in Fig. 1, and that to resolve finer details one needs to use C-AFM under liquid or NC-AFM. Another important observation is that after some time of exposure to water, it was generally not possible to image the PET surface. Even when imaging was possible, the surface appeared strongly deformed and by no means similar to the images obtained immediately after the introduction of the liquid. This observation was repeated several times, leading to the deduction that the PET surface is not stable under water, at least after several hours of exposure and in the depth of a few nanometers. Perhaps, more stable imaging can be obtained working under *n*-heptane. It seems that under liquid, the surface is generally not completely stable. This could be due either to tip dragging or to softening of the surface induced by the plastisizing effect of the liquid environment on the polymer. This issue was not further explored (and it was difficult to conclude whether the modification was reversible), and we concentrated on using NC-AFM, as the images obtained by non-contact mode are generally even better resolved than the images obtained under liquid. Although, the RMS roughness is not appreciably different from the C-AFM images, the texture appears more clear and detailed.

Fig. 3 shows NC-AFM images of two different BD film samples. They are presented to give evidence that on this type of film, the results are consistent. The typical texture is made of hillocks of 20 nm diameter on an average, with a RMS value ranging from 1 to 1.5 nm over a 1 μm^2 area. Larger lamella-like features were noticed on only one occasion and will be discussed in detail later (Fig. 6). They are not representative of the BD surface. The resolution strongly depends on the tip shape: it is essential for the tip to be sharp. Though one might find symmetries from any single image, no preferential direction can be identified after considering several images of the same sample. This is not surprising as the film was made by biaxial stretching in the machine (MD) and transverse (TD) directions. Other measurements made of the mechanical properties of these films did not show high anisotropy [34].

The observation of features of approximately 20 nm in size is consistent with previous structural studies on stretched PET films. For example, Chang et al. [8] have

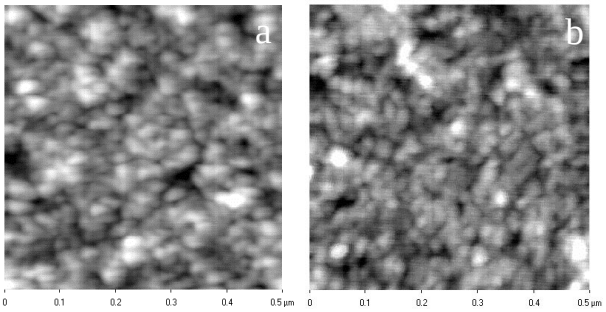

Fig. 3. BD PET film: (a) NC-AFM image, RMS = 0.9 nm; (b) NC-AFM image, RMS = 0.8 nm. The two images have been taken on different samples. The texture is very similar and in both cases hillocks of 20 nm diameter can be clearly seen.

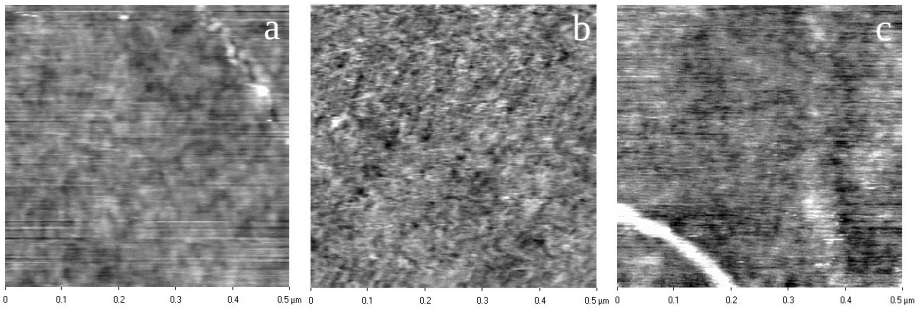

Fig. 4. Amorphous PET film: (a) C-AFM image in air at 0 nN load, RMS = 0.3 nm; (b) C-AFM image under water at 0 nN load, RMS = 0.4 nm; (c) NC-AFM image, RMS = 0.3 nm. The amorphous films are much smoother than the BD films. The texture appears featureless apart from the C-AFM images where a texture is noticeable, probably induced by tip dragging.

presented TEM images of biaxially stretched and annealed PET films. Their micrographs clearly show dark (crystalline) and bright (amorphous) areas of approximately the same size as the features observed by NC-AFM. We, therefore, believe that our NC-AFM images represent the genuine morphology of BD PET films. As mentioned previously, our attempt to apply UFM for BD films in order to distinguish the crystalline from the amorphous phase on the basis of the difference in their mechanical properties was unsuccessful. In most of the experiments, the polymer surface showed signs of modification by the scanning tip.

The analysis of the amorphous film by SPM showed that it is much smoother than the BD PET film with a RMS roughness of 0.3–0.4 nm. The texture appears featureless (Fig. 4). Some texture is noticeable in the C-AFM images; this texture was probably induced by scanning [19,20].

Fig. 5 shows C-AFM and NC-AFM images obtained for one of the HT samples (in this case at 120°C for 1 h). Taking a 1 μm^2 area, the HT samples are always much rougher than the untreated one. On a larger scale, the difference is even more marked. In these conditions, it is quite difficult to operate in NC-AFM as the tip occasionally comes into contact with the roughened surface (white "spikes" in Fig. 5). Apparently, the process of crystallisation produces enormous roughening of the surface. On the scale of our interest, $\sim$1 μm^2, the change in roughness due to heat treatment can be more than an order of magnitude.

Large lamella-like features were noticed on the surface of the HT samples (Fig. 6), but their presence proved rare. The lamella-like features, presented in Fig. 6, appear to be a few tens of nanometers in thickness and of varying length of the order of hundreds of nanometers. They could be identified with crystal lamellae edge-on. They are generally quite stable even in C-AFM in air. It is also possible to use modulation techniques for imaging local mechanical properties. In fact, these were the only regions in which UFM did not introduce any apparent damage on the surface.

Comparing the AFM results of the semicrystalline materials (BD and HT PET) investigated here with those of amorphous PET, it is obvious that crystallisation is associated with increase in the surface RMS values. Bearing in mind that for the HT samples, the rough lamellae features appear stable using UFM, we suggest that the lamella-like features represent the crystalline phase of PET. It seems plausible to draw an analogy between HT and BD films and make a preliminary suggestion that in Fig. 3, the observed hillocks represents small crystallites formed during the production process of BD films. Currently, we are continuing our investigations in order to verify this hypothesis with one direction is the high-resolution in situ NC-AFM imaging of a sample during annealing in the variable temperature set-up.

4. Conclusions

In order to image reliably the surface morphology of PET films, one needs to use NC-AFM in order to image fine details of the surface. To obtain a good resolution, the tip must be sharp enough, for example in order to resolve the hillocks on the BD films. C-AFM in air generally induces modification that, though shallow, prevents imaging of the real surface texture. The BD films can easily be damaged

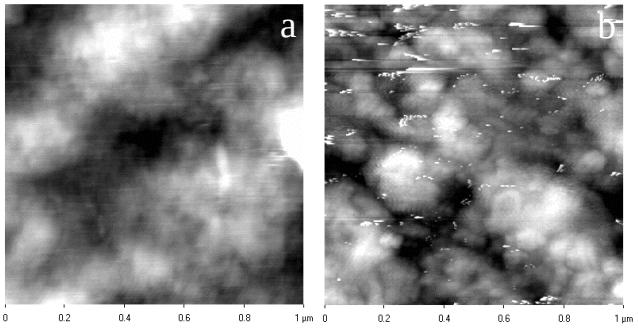

Fig. 5. HT PET film (at 120°C for 1 h): (a) C-AFM image in air at 0 nN load, RMS = 3.1 nm; (b) NC-AFM image, RMS = 4.7 nm. Taking a 1 μm^2 area, the HT film is much rougher than the amorphous one. On a larger scale, the difference is even more marked. NC-AFM can be very difficult to operate in such conditions. The white spikes are the result of the tip touching the surface during the scan. The process of crystallisation produces enormous roughening of the surface. On the scale of interest here, no feature identifiable with anything observed on the BD film, was observed.

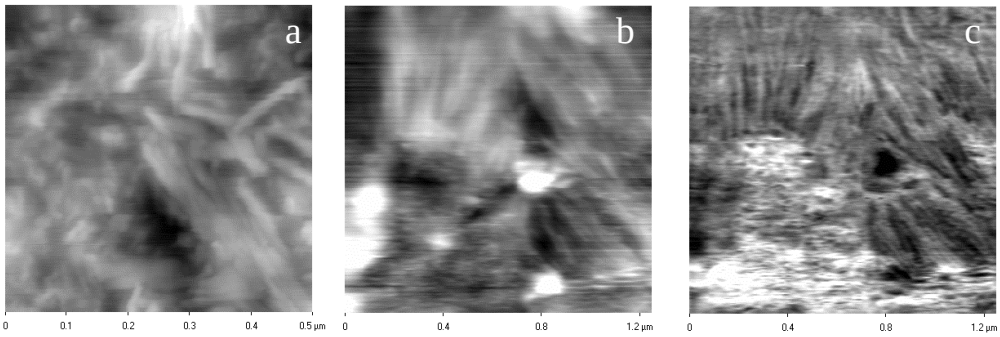

Fig. 6. (a) C-AFM image of HT PET film in air at 0 nN load: RMS = 3.9 nm. (b) C-AFM image of BD film in air at 0 nN load: RMS = 5.2 nm. (c) UFM image acquired simultaneously to image (b): brighter regions correspond to stiffer material. Such images have only been observed at a few points on the specimens examined. They are very stable even when using C-AFM in air and can be imaged using UFM. It can be noticed that the area with no lamella-like feature (bottom left of (b) and (c)) is clearly disrupted by contact imaging.

even under moderate load. Better results, almost as good as with NC-AFM, can be obtained by using C-AFM under water or *n*-heptane. In this case, a major drawback is represented by the fact that the PET surface is not stable to water exposure, even over a relatively short time (a few hours).

The observation that the BD films can be easily damaged suggests that in BD films in the near-surface region is, it either consists of small, defective, and therefore, with poor mechanical properties crystallites or is predominantly amorphous. The hillocks observed in the images of BD films could represent the crystalline phase whereas the area in-between could be amorphous. This speculation seems to be in accord with the roughening of the surface of PET upon heat induced crystallisation. However, further work is needed to prove this hypothesis.

Acknowledgements

This project was supported by Toppan Printing Company of Japan, within the Oxford Toppan Centre. O.V.K. would like to thank Paul Instrument Fund and EPSRC support (GR IL02234) for the development of the UFM. F.D. and O.V.K. would like to thank AFAM, CEC Network.

References

[1] Al Raheil IAM. Polym Int 1994;35:189–95.
[2] Fakirov S, Fischer EW, Hoffmann R, Schmidt GF. Polymer 1977;18:1121–9.
[3] Varma P, Lofgren EA, Jabarin SA. Polym Sci Engng 1998;38:237–53.
[4] Lapersonne P. Polymer 1991;32:3331–9.
[5] Blundell J, MacKerron DH, Fuller W, Mahendrasingam A, Martin C, Oldman RJ, Rule RJ, Riekel C. Polymer 1996;37:3303–11.
[6] Pearce R, Cole KC, Ajii A, Dumolin M. Polym Sci Engng 1997;37:1795–800.
[7] Koenig JL, Hannon MJ. J Macromol Sci, Phys B 1967;1:119–45.
[8] Chang H, Schultz JM, Gohil RM. J Macromol Sci, Phys B 1993;2:93–123.
[9] Yeh GSY, Geil PH. J Macromol Sci, Phys B 1967;1:235–49.
[10] Yeh GSY, Geil PH. J Macromol Sci, Phys B 1967;1:251–77.
[11] Binnig G, Quate CF, Gerber C. Phys Rev Lett 1986;56:930–3.
[12] Rugar D, Hansma PK. Phys Today 1990;43:23–30.
[13] Magonov SN, Reneker DH. Ann Rev Mater Sci 1997;27:175–222.
[14] Pearce R, Vancso GJ. J Polym Sci Part B, Polym Phys 1998;36:2643–51.
[15] Ivanov DA, Jonas AM. Macromolecules 1998;31:4546–50.
[16] Schultz JM, Miles MJ. J Polym Sci Part B, Polym Phys 1998;36:2311.
[17] Maivald P, Butt H-J, Gould SAC, Prater CB, Drake B, Gurley JA, Elings VB, Hansma PK. Nanotechnology 1991;2:103–6.
[18] Burnham NA, Gremaud G, Kulik AJ, Gallo P-J, Ouveley F. J Vac Sci Technol B 1995;14:1308–12.
[19] Gould SAC, Schiraldi DA, Occelli ML. J Appl Poly Sci 1997;65:1237–45.
[20] Ling JSG, Leggett GJ, Murray AJ. Polymer 1998;39:5913–21.
[21] Ling JSG, Leggett GJ. Polymer 1997;38:2617–25.
[22] Gould SAC, Schiraldi DA, Occelli ML. Chemtech 1998;28:35–9.
[23] Mate CM, McClelland GM, Erlandsson R, Chiang S. Phys Rev Lett 1987;59:1942–5.
[24] Fujihira M, Aoki D, Okabe Y, Takano H, Hokari H, Frommer J, Nagatani Y, Sakai F. Chem Lett 1996;7:499–500.
[25] Ando Y, Ino J. Sensors Actuators A 1996;57:83–9.
[26] Weisenhorn AL, Hansma PK, Albrecht TR, Quate CF. Appl Phys Lett 1989;54:2651–3.
[27] Kolosov O, Yamanaka K. Jap J Appl Phys Part 2, Lett 1993;32:L1095–8.
[28] Overney RM, Meyer E, Frommer J, Guntherodt H-J. Langmuir 1994;10:1281–6.
[29] Nie H-Y, Motomatsu M, Mizutani W, Tokumoto H. J Vac Sci Technol B 1995;13:1163–6.
[30] Overney R, Leta DP, Pictroski CF, Rafailovich MH, Liu Y, Quinn J. Phys Rev Lett 1996;76:1272–5.
[31] Dinelli F. PhD thesis, Oxford, 1998.
[32] Dinelli F, Assender HE, Takeda N, Briggs GAD, Kolosov OV. Sur Interface Anal 1998;27:562–7.
[33] Dinelli F, Biswas SK, Briggs GAD, Kolosov OV. Appl Phys Lett 1997;71:1177–9.
[34] Heras MP. PhD thesis, Oxford, Trinity 1998.